Journal Pre-proof

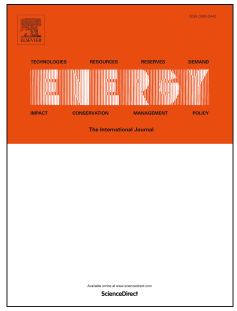

Combined pinch and mathematical programming method for coupling integration of reactor and threshold heat exchanger network

Di Zhang, Donghui Lv, Changfang Yin, Guilian Liu

PII: S0360-5442(20)31177-4

DOI: https://doi.org/10.1016/j.energy.2020.118070

Reference: EGY 118070

To appear in: *Energy*

Received Date: 14 January 2020

Revised Date: 21 May 2020

Accepted Date: 4 June 2020

Please cite this article as: Zhang D, Lv D, Yin C, Liu G, Combined pinch and mathematical programming method for coupling integration of reactor and threshold heat exchanger network, *Energy* (2020), doi: https://doi.org/10.1016/j.energy.2020.118070.

Credit author statement

Di Zhang: Conceptualization, Methodology, Software, Writing the draft;

Donghui Lv: Validation, Writing;

Changfang Yin: Software, Reviewing and Editing;

Guilian Liu: Investigation. Supervision.

Combined Pinch and Mathematical Programming Method for Coupling Integration of Reactor and Threshold Heat Exchanger Network

*Di Zhang, Donghui Lv, Changfang Yin, Guilian Liu**

(School of Chemical Engineering and Technology, Xi'an Jiaotong University, Xi'an, Shaanxi Province, 710049, China)

Abstract: A combined Pinch and Mathematical Programming Methodology is proposed to systematically integrate and optimize reactor and Threshold Heat Exchanger Network (HEN). With the reaction kinetics, mass balance and energy balance considered, the energy consumption of the Threshold HEN is analyzed based on the Composite Curves. Relations among the utility consumption of HEN, conversion and reactor temperature are deduced. With the Minimum Temperature Approach taken as variable and both capital and utility cost considered, a Mixed Integer Nonlinear Programming (MINLP) model is developed to integrate HEN and reactor. Based on this model, the maximum net annual revenue and utility consumptions at different conversions can be identified, as well as the corresponding inlet and outlet temperature of reactors and Minimum Temperature Approach. A duty-annual revenue-conversion-temperature ($\dot{Q}$-Y_{NAR}-X-T) diagram is constructed to illustrate their variation, and intuitively target the optimal conversion and corresponding parameters. A steam-reforming process is studied by the proposed method. The optimal conversion of the reactor is identified to be 0.84, and the net annual revenue can be increased by 27.82% after the optimization.

Key words: reactor; integration; heat exchanger network; threshold problem;

*Corresponding author: Prof. Guilian Liu, E-mail: guilianliui@mail.xjtu.edu.cn.

optimization

1 Introduction

Due to the development of world economy in recent years, the decrease of fossil energy reserves and its low energy efficiency are getting more prominent [1]. Currently, fossil fuel still dominates the world's energy consumption, and this situation is expected to continue over the next decades. In 2018, the chemical process is responsible for 73 % of global fossil energy consumption [2]. While its energy efficiency is quite low, as a large amount of energy is lost, sometimes even up to 50 % [3]. Because of this, there is a significant potential to recover energy by integration [4].

Reactor is the core of the chemical process and transforms reactants into desired products and byproducts. Its feed and product are generally the sources or/and sinks of the Heat Exchanger Network (HEN); its parameters affect their compositions, flowrates and temperatures, as well as the Composite Curves [5] and energy consumption of HEN [6].

The HEN can be classified into Pinch Problem and Threshold Problem [7]; the effect of reactor parameters on them are different. For the Pinch Problem, which consumes both heating and cooling utilities, the variation of reactor parameters affects both utilities. While for the Threshold Problem, which demands only the heating or cooling utility, the reactor parameters affect the distribution of the utility demand. Sometimes, the threshold HEN might transform into the Pinch Problem, and vice versa. In addition, reactor parameters affect the heat exchanger area and total cost of the HEN. To reduce the energy consumption and total cost, it is necessary to target the optimal reactor parameters and the minimum energy consumption of HEN based on their integration.

Pinch Analysis (PA) originally emerged as an approach to target the maximum heat recovery of HENs [8]. In this method, utility targets are identified based on the thermodynamic principles, and detailed HEN is designed with the aid of the decomposition strategy [9]. A variety of pinch-based methods are proposed to deal with HENs with different characteristics. A modified pinch approach was introduced by Bakhtiari and Bedard [10] to handle complex network configurations with stream segmentation and splitting. Based on the plot of hot streams' temperatures versus cold streams' temperatures, Gadalla [11] presented a new graphical method to identify the exchangers across the pinch and the improper placement of fuel consumption. This method can be applied to modify the existing networks for reducing the fuel demands. Kang et al [12] presented a *T-Q* diagram to integrate large-scale HENs with matching difficulties reduced. Li et al [13] proposed a visualized *T-H* diagram for the identification of cross-pinch heat transfer with phases change. In recent years, PA method has been extended to different systems, such as Work Exchange Network [14], Hydrogen Integration [15], Water Network [16] and Carbon Footprint visualization [17].

Since Threshold HEN demands only one type of utility, it has the characteristics different from the Pinch Problem [18]. In the synthesis and optimization of HEN, Threshold Problem is generally taken as a special case of Pinch Problem [19]. More often, its study mainly focus on the energy-saving measures of specific production process [20]. Based on the Pinch Method, Panjeshahi et al [21] analyzed the HEN of an ammonia synthesis plant and proposed an optimization scheme to transfer the HEN into a threshold one. Ashkan and Mehdi [22] studied the feasible energy integration of a soot production cycle and indicated that the furnace is the best source to provide the heating utility of this Threshold HEN. Wang et al [23] analyzed the energy consumption of the subsequent process in an acetic acid cracking plant, whose HEN is a Threshold Problem, and proposed two energy-saving projects to reduce the cooling utility by 40 %. Sun et al [24] considered the parallel and countercurrent flows in the multi-pass HEN and dealt with the matches of process streams for multi-pinch and threshold HEN.

Besides PA, Mathematical Programming (MP) is also a successful basis for the synthesis and retrofit of HEN. It has a fair degree of automaticity to solve large and complex HENs [25]. In the crude distillation unit of a refinery, a mathematical model was designed by Srikanth et al [26] to optimize the Threshold Temperature Approach for complex HENs. Based on a step-wise superstructure and hybrid genetic algorithm, another crude distillation unit was integrated to identify the optimal Threshold Temperature Approach with the best performance of the HEN [27]. Later, a Segregated Problem Table Algorithm (SePTA) was introduced by Wan Alwi and co-workers [28] for simultaneous targeting and design of HEN, and this method can be applied to systems with multiple Pinches and Threshold Problem. Besides, methods proposed for the optimization of general HEN can also be used to solve the Threshold Problem, such as the hybrid chaotic ant swarm algorithm [29], stage-wise based superstructure [30], the methodology considering the performance of reused heat exchange units [31], the stream temperature versus enthalpy plot retrofit method [32], Monte Carlo Simulation (MCS) method [33], etc. These methods can consider the use of splits, cross flows, heat exchanger allocation, diagnosis and retrofit of existing HEN, and the effect of stream data variation. Furthermore, methods are developed with the trade-off between efficiency and capital costs considered seriously, such as the Mixed Integer Nonlinear Programming (MINLP) approach for simultaneous synthesis of HENs and Utility Systems [34] and that with all possible HEN configurations and multiple utilities [35], the fuzzy-Analytic Hierarchy Process (AHP) model [36], the transshipment type model [37], flexible HENS methodology considering the influence of fouling [38], optimization-based framework for designing dynamic flexible HENs [39].

In order to combine the advantages of both methods together, Pinch Analysis method can be integrated with the Mathematical Programming method [40]. Zhang et al [41] established an optimization algorithm based on the Cuckoo Search Algorithm and applied it to solve both Pinch and Threshold Problems. Considering the trade-off between the operating and capital costs, the effect of Minimum Temperature Approach and multiple utilities, Sun et al [42] proposed a method to design the cost-effective HEN. Bakar et al [43] proposed the guide for selecting the optimal Minimum Temperature Approach of flexible and operable HEN. Through the research introduced above, the integration between HEN and reactors are out of the consideration.

In view of reactors, Glavič et al [44] studied its integration with HEN and developed a method for identifying its proper placement. Later, this method was applied to match streams with energy-active equipment [45]. Tian et al [46] studied the integration between the hydrotreating reactor and HEN, and analyzed the effect of catalyst deactivation on the energy consumption. Director and Sinelshchikov [47] developed a one-dimensional mathematical model for simulating the reactor with the direct heating and recirculation of heat carrier. A biochar production process with pyrolysis reactor integrated with boiler is introduced by Kim et al [48]. In this process, the flue gas is extracted as a heat source of HEN. Zhang et al developed an integration-based sensitivity analysis methodology to integrate HEN with Continuous Stirred Tank Reactor (CSTR) [5] and Plug Flow Reactor (PFR) [6], and target the optimal reactor parameters.

The Threshold HEN demands only one type of utility and has the characteristics different from the Pinch Problem. When the Minimum Temperature Approach and reactor parameters change, different amounts of high-temperature or low-temperature utilities might be used, and the trade-off between the utility cost and capital cost is different from that of the pinch problem. In addition, the product profit changes along reactor parameters. It is necessary to develop a systemic method for integrating the Threshold HEN and reactor and analyzing the trade-off between utility and capital costs. According to the literature survey and to the best of the author's knowledge, no report concentrates on this problem.

This paper aims to develop a combined Pinch Analysis and Mathematical Programming method to integrate reactor and Threshold HEN, optimize the reactor parameters and target the Minimum Temperature Approach. The variation of the utility consumption will be deduced first based on Pinch Analysis. Then the relation between inlet/outlet temperatures and reactor conversion is analyzed. Based on this, the Mathematical Programming model is developed to systematically integrate reactor and Threshold HEN, and target the optimal reactor parameters and Minimum Temperature Approach. A steam-reforming process will be studied to illustrate the application of the proposed method.

2 Methodology

2.1 Problem Statement

Reactor's feed and product are generally the sources or/and sinks of the HEN. Its parameters affect their compositions, flowrates and temperatures, as well as the integration of the HEN. The Threshold HEN demands only one type of utility. When the Minimum Temperature Approach and reactor parameters change, different amounts of high-temperature or low-temperature utilities might be used, and the trade-off between the utility cost and capital cost is different from that of the pinch problem.

This work aims to study the integration between Threshold HEN and reactor, and develop a combined Pinch Analysis and Mathematical Programming method for optimizing the Minimum Temperature Approach and reactor parameters simultaneously. The relation between the utility consumption of HEN and reactor parameters are the basis of integration, and will be deduced according to reaction kinetics, mass and energy balance, and the topology of HEN. With the variation of heat recovery and product profit taken into account, mathematical model will be constructed to target the optimal reactor parameters and the optimal Minimum Temperature Approach. The objective of the optimization is to maximize the net annual revenue.

2.2 Characteristics of Threshold HEN and Effect of Reactor Temperature

2.2.1 Characteristics of Threshold HEN

In the HEN, the Minimum Temperature Approach (ΔT_{min}) is a critical parameter for both Pinch and Threshold Problem. Its selection needs to consider the trade-off between utility and capital costs. In optimization, the lower boundary of the Minimum Temperature Approach can be set according to the operational flexibility.

For Threshold HEN, its demand on heating utility is zero and that on cooling utility is $\dot{Q}_{\mathrm{Cmin}}$, as shown in Fig. 1 (a), or vice versa. When the consumption of one utility just decreases to zero, the corresponding Minimum Temperature Approach is the Threshold Temperature Approach and denoted by ΔT_{THR}. Along with the decrease of ΔT_{min}, two Composite Curves get closer; the utility ($\dot{Q}_{\mathrm{Cmin1}}$) decreases at one end, while the demand for the same type of utility ($\dot{Q}_{\mathrm{Cmin2}}$) increases at the other end, as shown by Fig. 1 (b); the total utility ($\dot{Q}_{\mathrm{Cmin}}=\dot{Q}_{\mathrm{Cmin1}}+\dot{Q}_{\mathrm{Cmin2}}$) is a constant [7] as the increment and decrement of utilities are the same.

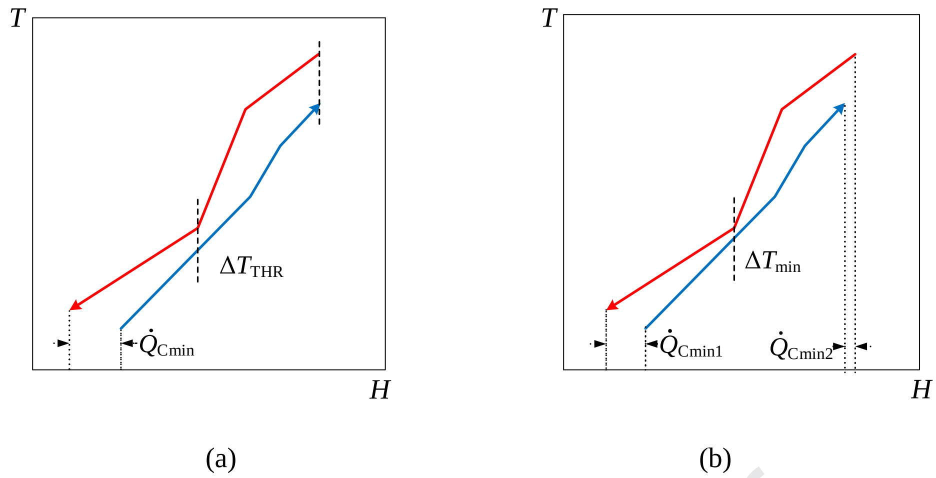

Fig. 1 Composite Curves with different relative locations

In Fig. 1, it can be indicated that when $\Delta T_{min} \leq \Delta T_{THR}$, the total utilities do not change with the Minimum Temperature Approach and the utility cost is fixed. When $\Delta T_{min} > \Delta T_{THR}$, the HEN turns to be a Pinch Problem. In this case, the utility cost is proportional to ΔT_{min}. The Optimal Temperature Approach corresponding to the minimum total cost might appear at or above the Threshold Temperature Approach, as shown by Fig. 2. It can be identified with the trade-off between capital cost and utility cost considered [7].

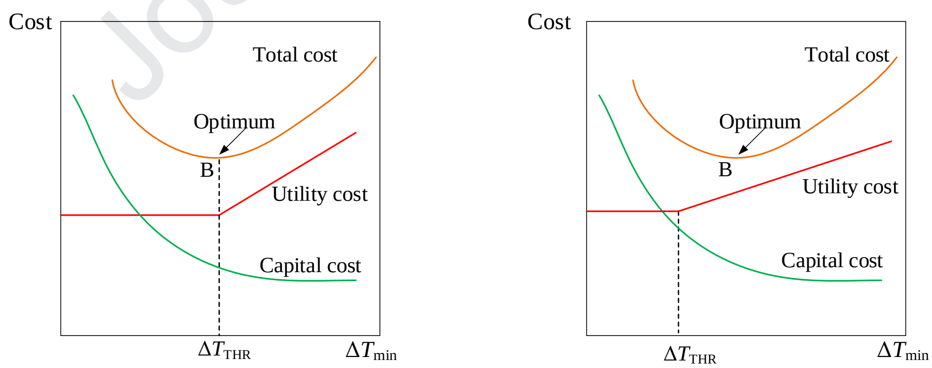

(a) The optimum point appears at ΔT_{THR} (b) The optimum point appears above ΔT_{THR}

Fig. 2 The trade-off between utility and capital cost along ΔT_{min}

Although the total demands on heating and cooling utilities keep unchanged for Threshold Problem, their cost varies along ΔT_{min}, as their prices at different temperatures are diverse. For example, for the system shown in Fig. 1 (b), the energy at the hot end is released at a high temperature and can be used for generating steam; while that at the cold end can only be cooled by the cooling water. With both the cooling water consumption and steam generation considered, the variation of utility cost along $\Delta T_{\min}$ is no longer a flat profile, as shown in Fig. 3. In this case, the Optimal Temperature Approach may appear below ΔT_{THR}.

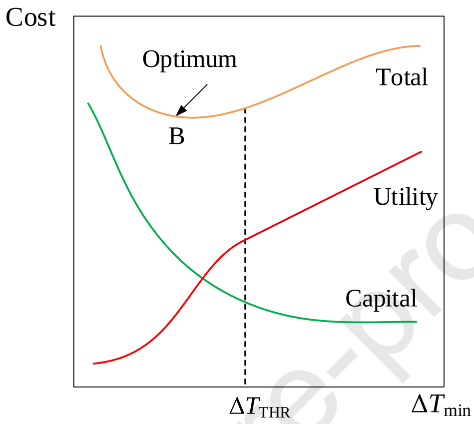

Fig. 3 Variation of cost along $\Delta T_{\min}$

2.2.2 Effect of Reactor Temperature on Utility Distribution

For a reactor, its feed usually needs to be preheated and corresponds sink SK_q, while its product is generally a source represented by SR_p. Its inlet temperature corresponds to the target temperature of SK_q, and its outlet temperature is the supply temperature of SR_p. These temperatures change along the reactor's operating parameters, and affect the Composite Curves and energy consumption [6].

In a HEN, there are multiple sources and sinks. The supply/target temperature of each stream corresponds to an inflexion point of the Composite Curve, and is a possible bottleneck of the HEN in terms of energy recovery. The Threshold Problem shown in Fig. 4 is taken as an illustrative example to analysis this situation. In this temperature-heat flow diagram, Source Composite Curve and Sink Composite Curve are ABCDEFG and HIJKLM, respectively. Point A and H have the same horizontal ordinate; the Threshold Temperature Approach corresponds to point D, which lies at the middle of Composite Curves, and the minimum cooling utility is $\dot{Q}_{\text{Cmin}}$ (Note, to avoid the confusion with the thermodynamic term, enthalpy (kJ/kg), heat flow is used to indicate the heat content of a stream (kW)).

If the target temperature of sink SK_q increases from T_1 to T_1', the variation of the heating duty demanded by cold streams (ΔH_1) can be calculated by Eq. (1) [6]. Besides, the supply temperature, flow rate and/or composition of SR_p will change, as well as its CP. In Fig. 4, the supply temperature of SR_p increases from T_2 to T_2', and line CB changes to CB″. B′B″ stands for the variation due to that of CP (ΔCP); AA″ is the increment of this source's cooling duty (ΔH_2), and can be calculated by Eq. (2) [6]. The sink and source Composite Curves change into H′I′J′JKLM and A″B″CDEFG accordingly.

$$\Delta H_1 = CP_{SK_q}\left(T_1' - T_1\right) \tag{1}$$

$$\Delta H_2 = CP_{SR_p}\left(T_2' - T_2\right) + \Delta CP\left(T_2' - T_C\right) \tag{2}$$

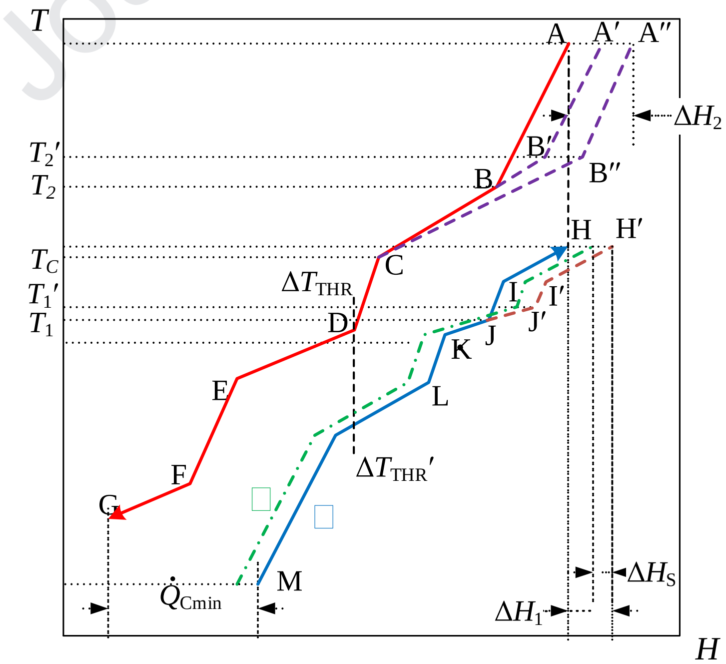

Fig. 4 Variation of Composite Curves when the heating utility is zero

When the temperatures of SR_p and SK_q change, the variation of utilities can be targeted according to the method introduced in Ref. [6]. If T_1, T_1', T_2 and T_2' lie above the Threshold Temperature, the variation of cooling utility ($\Delta\dot{Q}_{\mathrm{CL}}$) is 0, and that of the heating utility ($\Delta\dot{Q}_{\mathrm{HT}}$) can be calculated by Eq. (3).

$$\Delta\dot{Q}_{\mathrm{HT}} = \Delta H_1 - \Delta H_2 \tag{3}$$

If $\Delta\dot{Q}_{\mathrm{HT}}$ is positive, the HEN changes from Threshold Problem into Pinch Problem. Otherwise, the HEN is still a Threshold Problem; the surplus energy at the hot end equals $\Delta\dot{Q}_{\mathrm{HT}}$ ($=\Delta H_2 - \Delta H_1$), and can be cooled by cooling utility with higher temperature or be reused to generate steam.

If the Minimum Temperature Approach is reduced, the Sink Composite Curve should be shifted leftward by ΔH_{S}. In this situation, the variation of cooling and heating utilities are shown by Eq. (4) and Eq. (5), respectively.

$$\Delta\dot{Q}_{\mathrm{CL}} = -\Delta H_{\mathrm{S}} \tag{4}$$

$$\Delta\dot{Q}_{\mathrm{HT}} = \Delta H_1 - \Delta H_2 - \Delta H_{\mathrm{S}} \tag{5}$$

For systems with the Threshold Temperature Approach located at the hot or cold end, and the inlet/outlet streams of the reactor have different source/sink belongingness, the variation of heating and cooling utilities can be analyzed by the same method, and the results are listed in Table 1. In this table, ΔH_1 and ΔH_2 are the duty variation of SK_q and SR_p, respectively; ΔH_{S} is the distance of the Sink Composite Curve shifted leftward.

Table 1 Utility variations for exothermic reaction

Position of SK_q and SR_p	Heating utility is 0		Cooling utility is 0	
	$\Delta\dot{Q}_{HT}$	$\Delta\dot{Q}_{CL}$	$\Delta\dot{Q}_{HT}$	$\Delta\dot{Q}_{CL}$
Both Above the threshold point	$(\Delta H_1\text{-}\Delta H_2)\text{-}\Delta H_S$	$\text{-}\Delta H_S$	$(\Delta H_1\text{-}\Delta H_2)\text{-}\Delta H_S$	$\text{-}\Delta H_S$
Both below the threshold point	$\text{-}\Delta H_S$	$(\Delta H_2\text{-}\Delta H_1)\text{-}\Delta H_S$	$\text{-}\Delta H_S$	$(\Delta H_2\text{-}\Delta H_1)\text{-}\Delta H_S$
Across the threshold point	$\text{-}\Delta H_2\text{-}\Delta H_S$	$\text{-}\Delta H_1\text{-}\Delta H_S$	$\text{-}\Delta H_2\text{-}\Delta H_S$	$\text{-}\Delta H_1\text{-}\Delta H_S$

When the inlet and outlet temperatures of the reactor change, the pinch might appear. Fig. 5 illustrates the composite curves of a Threshold HEN; its heating utility is zero. In this HEN, a pair of hot and cold streams (SR_p and SK_q) are connected to an endothermic reaction. When the inlet temperature of SK_q (corresponding to point H) increases from T_1 to T_1' and the outlet temperature of SR_p (corresponding to point C) increases from T_2 to T_2', the Minimum Temperature Approach lies at point C′. If the increment of the energy demanded by the sinks (ΔH_1) is greater than that released by the sources (ΔH_2), the HEN turns into a Pinch Problem. The Pinch Problem can be transferred into the Threshold Problem through reducing the Minimum Temperature Approach and shifting two Composite Curves closer.

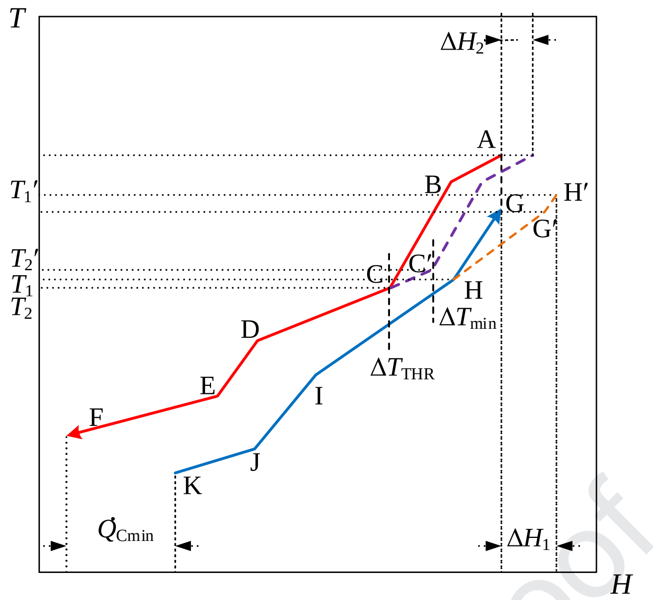

Fig. 5 Threshold HEN turns into Pinch Problem after increasing the reactor's temperatures

2.2.3 Relationship between the Conversion and Temperature of Reactor

A reversible reaction with components B and D reacted to product S and W is shown below:

$$B + dD \rightleftharpoons sS + wW$$

Where, B is the key component and this is applicable to all equations in this paper; *d*, *s* and *w* are the stoichiometric coefficients of species D, S and W, respectively.

If the reaction is processed in a CSTR reactor, the mass balance for this reactor can be represented by Eq. (6) [5].

$$\frac{F_{\mathrm{B}}^{0} \cdot X}{V \cdot A} = \exp\left(\frac{E}{RT}\right) \prod c_i^{\alpha_i} \quad (6)$$

Where, X is the conversion of key species B; F_i, c_i and α_i stand for the flow rate, mole concentration and reaction order of species i, respectively. Superscript 0 denotes the parameter is that at inlet condition; E and A are the activation energy and pre-exponential factor, respectively, and are affected by the catalyst; V and T denote the volume and the outlet temperature of the reactor; R is the ideal gas constant which is usually taken as 8.314 $\mathrm{J \cdot mol^{-1} \cdot K^{-1}}$.

The mole concentration for each component is described by Eq. (7).

$$c_i = c_i^0 + \xi_i c_{\mathrm{B}}^0 \cdot X \tag{7}$$

Where, ξ_i is stoichiometric coefficient of species i.

For a given catalyst, the pre-exponential factor (A) and the activation energy (E) can be taken as unchanged within a certain temperature interval [49]. Eq. (8) shows the relation between reaction temperature (T) and the conversion (X) of key species B [6].

$$\frac{F_{\mathrm{B}}^0 \cdot X \cdot \left(c_{\mathrm{B}}^0\right)^{-\sum\alpha_i}}{V \cdot A} = \exp\left(\frac{E}{RT}\right)\prod\left(\frac{c_i^0}{c_{\mathrm{B}}^0} - \xi_i X\right)^{\alpha_i} \tag{8}$$

While for gas phase reaction, the concentration is influenced by both temperature and pressure of the reactor [49]. According to the gas state equation, Eq. (8) is revised into Eq. (9).

$$\frac{F_{\mathrm{B}}^0 \cdot X \cdot \left(c_{\mathrm{B}}^0 \cdot \frac{T_0}{T} \cdot \frac{P}{P_0} \cdot Z\right)^{-\sum\alpha_i}}{V \cdot A} = \exp\left(-\frac{E}{RT}\right)\prod\left(\frac{c_i^0}{c_{\mathrm{B}}^0} - \xi_i X\right)^{\alpha_i} \tag{9}$$

Where, T_0 and P_0 represent the temperature and pressure at the inlet condition; P stands for the pressure of the reactor; Z is the compression factor of gas.

For gas phase reaction, if the partial pressure is used instead of mole concentration, Eq. (9) can be written into Eq. (10).

$$\frac{F_{\mathrm{B}}^0 \cdot X}{V \cdot A} = \exp\left(\frac{E}{RT}\right)(1-\omega)\prod P_i^{\alpha_i} \tag{10}$$

Where, ω is the reversibility factor reflecting the effect of the reverse reaction on the gas reaction rate [50]. It is determined by the experiment and varies slightly along pressure and temperature, and can be taken as a constant [51]. P_i denotes the partial pressure of species i in the reactor, and can be calculated by Eq. (11).

$$P_i = y_i \cdot P = P \cdot \frac{F_i^0 + \xi_i F_{\mathrm{B}}^0 X}{F} \tag{11}$$

Where, y_i is the mole fraction of species i, and F denotes the total inlet molar flow rate of the reactor.

Based on Eq. (11), Eq. (10) is modified into Eq. (12).

$$\frac{F_{\mathrm{B}}^{0} \cdot X \cdot \left(P^{total}\right)^{-\sum \alpha_i}}{V \cdot A} = \exp\left(\frac{E}{RT}\right)(1-\omega)\prod y_i^{\alpha_i} \tag{12}$$

In addition to the mass balance, the energy balance of the reactor is considered. For an adiabatic CSTR reactor, it is shown by Eq. (13).

$$\dot{Q}_{\mathrm{R}} - \sum\left(F_i^0 \cdot Cp_i\right)\left(T - T_0\right) - \left[\Delta H_{Rx}^{\Theta}\left(T_{\mathrm{R}}\right) + \sum\left(-\xi_i Cp_i\right)\cdot\left(T - T_{\mathrm{R}}\right)\right] F_{\mathrm{B}}^{0} X = 0 \tag{13}$$

Where, Cp_i denotes the heat capacity of species i; $\Delta H_{Rx}^{\Theta}\left(T_{\mathrm{R}}\right)$ is the standard reaction heat at the reference temperature, T_{R}; $\dot{Q}_{\mathrm{R}}$ stands for the energy supplied to the reactor, and equals zero for adiabatic reactor.

Eq. (8) and Eq. (12) are derived based on mass balance, and can be applied to identify the relation between conversion (X) and temperature (T) for liquid and gas phase reactions, respectively. Eq. (13) shows the relationship among conversion (X), inlet (T_0) and outlet temperature (T) of the reactor. When the reactor's parameters are adjusted, the variation of its conversion depends on the thermodynamic, reaction equilibrium and kinetics, and is associated with the inlet and outlet temperatures of the reactor. Their relation can be identified with Eq. (8) (or Eq. (12)) and Eq. (13) combined.

2.3 Optimization of Reactor and HEN

A reactor's parameters affect the Composite Curves and the energy consumption, as its feed and product are the sink/source streams of the HEN. To optimize the reactor and HEN and maximize the annual revenue, the capital cost is considered together with the utility cost, and a mathematical model and optimization flowsheet will be built in this section.

2.3.1 Mathematical Model

The relation among conversion (X), inlet (T_0) and outlet temperature (T) of the reactor are illustrated by Eq. (8), Eq. (9), Eq. (12) and Eq. (13). When the conversion changes from X to X', the corresponding inlet and outlet temperatures of the reactor changes to T_0' and T', which can be identified through solving these equations. The energy demands of the inlet and outlet stream of the reactor are calculated by Eq. (1) and Eq. (2), and that of utilities can be determined according to Table 1. At different conversions, the coordinates corresponding to each inflexion point of the Composite Curves can be obtained according to its original coordinate and the variation of utilities. Based on this, an MINLP model is proposed to estimate the heat transfer area and utility consumptions at different Minimum Temperature Approaches.

The Composite Curves of Threshold HEN are divided into vertical heat flow intervals by the vertical lines plotted at each inflection point, as shown by Fig. 6 (a) [52]. In this figure, j denotes the vertical heat flow interval, and J is the total number of intervals. Fig. 6 (b) shows part of the Source and Sink Composite Curves of Fig. 6 (a). The hot streams in interval j releases heat $\Delta\dot{Q}_j$, and its temperature decreases from T_{j+1} to T_j, while the cold streams in this interval absorbs the heat directly and their temperature increases from t_j to t_{j+1}. The utility is used in interval 1 and interval J. Based on the previous analysis, an MINLP model is built to calculate the utility consumption and target the heat transfer area simultaneously.

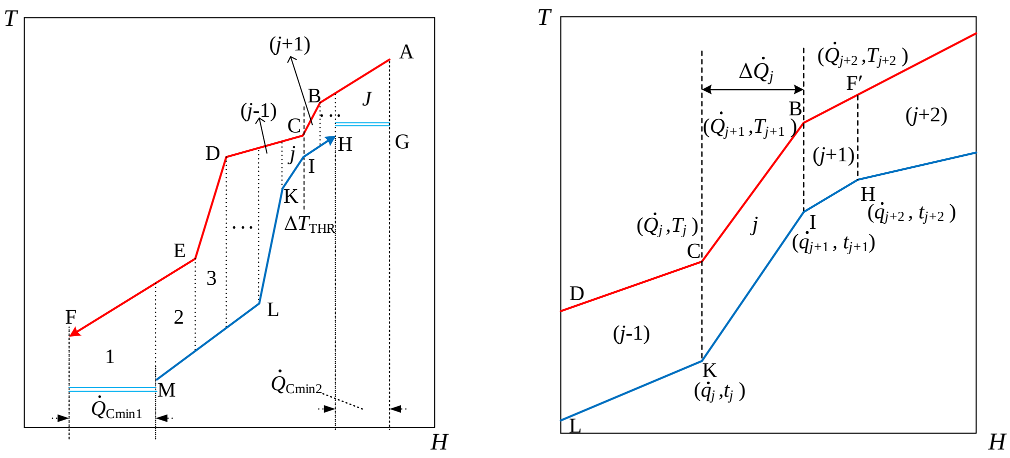

(a) Original Composite Curves (b) Heat exchange in a heat flow interval

Fig. 6 Vertical heat flow intervals of Composite Curves

The definitions and constrains are as follows:

Capital cost

For the vertical heat transfer interval j in Fig. 6 (b), coordinates of point B and C are $(\dot{Q}_{j+1}, T_{j+1})$ and $(\dot{Q}_j, T_j)$, and corresponds to the supply and target temperatures of hot stream, respectively; while I and K correspond to the target and supply temperatures of cold stream and their coordinates are $(\dot{q}_{j+1}, t_{j+1})$ and $(\dot{q}_j, t_j)$, respectively. In each interval, the heat balance is represented by Eq. (14). The heat transfer is restricted by Eq. (15)~Eq. (18), and the Logarithmic Mean Temperature Difference (*LMTD*) can be calculated by Eq. (19).

$$\Delta\dot{Q}_j = \dot{Q}_{j+1} - \dot{Q}_j = \dot{q}_{j+1} - \dot{q}_j, \quad 1 \le j \le J \tag{14}$$

$$T_{j+1} > T_j, \quad 1 \le j \le J \tag{15}$$

$$t_{j+1} > t_j, \quad 1 \le j \le J \tag{16}$$

$$T_j > t_j, \quad 1 \le j \le J \tag{17}$$

$$T_{j+1} > t_{j+1}, \quad 1 \le j \le J \tag{18}$$

$$LMTD_j = \frac{\left(T_{j+1} - t_{j+1}\right) - \left(T_j - t_j\right)}{\ln \dfrac{T_{j+1} - t_{j+1}}{T_j - t_j}}, \quad 1 \le j \le J \tag{19}$$

In each heat flow interval of the Composite Curves, the temperature differences should not be less than the Minimum Temperature Approach (ΔT_{min}) of the process. When the Sink Composite Curve is shifted leftward, the intervals need to be redistributed. On the Sink Composite Curve, the heat flow of the point corresponding temperature (t) can be determined by Eq. (20). Based on the assumption that there is the countercurrent and vertical heat transfer between sources and sinks in each heat flow interval, the temperature differences on both sides of interval j are restrained strictly by Eq. (21) and Eq. (22); the total heat transfer area ($Area$) equals the sum of those in all intervals ($Area_j$), as shown by Eq. (23) [52].

$$\dot{q}_j = \dot{q}_j - \Delta H_{\mathrm{S}} \tag{20}$$

$$T_{j+1} - t_{j+1} \ge \Delta T_{\mathrm{min}} \tag{21}$$

$$T_j - t_j \ge \Delta T_{\mathrm{min}} \tag{22}$$

$$Area = \sum Area_j = \sum \frac{\dot{Q}_{j+1} - \dot{Q}_j}{K_j \cdot LMTD_j} = \sum \frac{\dot{q}_{j+1} - \dot{q}_j}{K_j \cdot LMTD_j} \tag{23}$$

Where, K_j is the overall heat transfer coefficient in heat flow interval j.

When the temperature approaches or the reactor parameters change, the heat transfer area ($Area$) in some intervals will change. This affect the annualized capital cost. In order to optimize the system accurately and reasonably, the capital cost of heat exchanger should be considered in the model.

For the system with the reactor given, the capital cost mainly consists the purchase cost and the installation cost of heat exchangers [53]. The purchase cost is influenced by heat exchanger area, which can be predicted according to the Composite Curves

[54]; while the installation cost, Y_{eq}, is estimated according the purchase cost and the installation factor [55].

When the Minimum Temperature Approach between sources and sinks or the temperatures related to reactor are adjusted, the vertical intervals need to be redistributed, and the heat exchange area should be amended from *Area* to *Area'*. The increment of annual capital cost (Y_{IAC}) can be calculated by Eq. (24).

$$Y_{IAC} = \frac{Y_{\mathrm{eq}} + z\left(a + bArea'^{u}\right) - \left(a + bArea^{u}\right)}{D_{\mathrm{P}}} \tag{24}$$

Where, D_{P} is the depreciable period for heat exchangers; a, b and u are constants related to heat exchanger cost; z is the installation factor of heat exchanger, which is an empirical constant in different processes.

Heat recovery

When the Composite Curves get closed to each other, the demands on the utilities at different levels change accordingly. Based on the relation between the decrement of utilities and the Minimum Temperature Approach, the annual heat recovery (Y_{AHR}) is represented by Eq. (25). In this equation, $\Delta\dot{Q}_{\mathrm{CL}}$ and $\Delta\dot{Q}_{\mathrm{HT}}$ are identified according to Table 1; $\sum\left(\frac{\left|\Delta\dot{Q}_{\mathrm{HT}}\right|\cdot J_{\mathrm{S}}}{W_{\mathrm{S}}}\right)$ and $\sum\left(\frac{\left|\Delta\dot{Q}_{\mathrm{CL}}\right|\cdot J_{\mathrm{C}}}{W_{\mathrm{C}}}\right)$ stand for the sum of heating and cooling utility revenue per unit time (USD·h^{-1}), respectively; $\frac{\left|\Delta H_{\mathrm{S}}\right|\cdot J_{\mathrm{Q}}}{W_{\mathrm{Q}}}$ stands for the benefit recovered from the steam (USD·h^{-1}): D_{T} is the annual operating time of the process.

$$Y_{AHR} = \left[\sum\left(\frac{\left|\Delta\dot{Q}_{\mathrm{HT}}\right|\cdot J_{\mathrm{S}}}{W_{\mathrm{S}}}\right) + \sum\left(\frac{\left|\Delta\dot{Q}_{\mathrm{CL}}\right|\cdot J_{\mathrm{C}}}{W_{\mathrm{C}}}\right) + \frac{\left|\Delta H_{\mathrm{S}}\right|\cdot J_{\mathrm{Q}}}{W_{\mathrm{Q}}}\right] D_{\mathrm{T}} \tag{25}$$

Product profit variation

A reactor's conversion changes along its operating parameters, inlet and outlet temperatures. The annual profit variation (Y_{APV}) of the product is described by Eq. (26).

$$Y_{APV} = F_{\mathrm{B}}^{0} \cdot J_{\mathrm{P}} \cdot \left(X' - X \right) \cdot D_{\mathrm{T}} \tag{26}$$

Where, X' is the conversion after the reactor parameters are adjusted.

Objective function

In the integration of reactor and HEN, the increment of annual capital cost (Y_{IAC}), annual heat recovery (Y_{AHR}) and the annual profit variation of product (Y_{APV}) are considered together. The objective is to maximize the net annual revenue (Y_{ANR}), as shown by Eq. (27).

$$\max Y_{ANR} = Y_{AHR} + Y_{APV} - Y_{IAC} \tag{27}$$

In this equation, the increment of annual capital cost (Y_{IAC}) is taken away from the sum of annual heat recovery (Y_{AHR}) and the annual profit variation of product (Y_{APV}). Decreasing the annualized capital cost and increasing Y_{AHR} and Y_{APV} can benefit the performance of the system.

2.3.2 Optimization Procedure

Based on the model introduced in Section 4.1, the Threshold HEN can be integrated with CSTR reactor; the Minimum Temperature Approach at different conversions is optimized, and the optimal one (ΔT_{OP}) can be identified; the maximum net annual revenue and the corresponding ΔH_{S} are identified. The identification procedure is shown in Fig. 7. In this procedure, the reactor is assumed to be operated in conversion interval [X_m, X_n], and this interval is divided into l sub-intervals averagely.

The mathematical model can be solved by Matlab software [56]. According to the results, the $\dot{Q}$-Y_{NAR}-X-T diagram is plotted to illustrate the relationship among conversion, temperature, utility consumption and the corresponding optimal net annual revenue, as shown by Fig. 8. In this figure, two vertical axis on the left stand for the absolute value of the utility consumption and the net annual revenue; while those on the right side correspond the temperature of the reactor and the Optimal Temperature Approach. $\dot{Q}_{UCC}$ and $\dot{Q}_{UCH}$ stand for the surplus or deficit of utilities at cold and hot ends.

For the reactor operated within conversion interval [X_C, X_D], the maximum revenue and the corresponding reactor parameters to achieve this revenue can be identified easily from this figure. For example, for a given conversion X_A, the corresponding maximum net annual revenue (Y_A, point A_1), outlet and inlet temperatures (T_A, point A_2; T_{0A}, point A_3), cooling and heating utilities ($\dot{Q}_{1A}$, point A_4; $\dot{Q}_{2A}$, point A_5), and the Optimal Temperature Approach ($\Delta T_{OP,A}$) are identified. This figure shows clearly that point B_1 corresponds the optimal revenue, Y_B, and the corresponding Optimal Temperature Approach is $\Delta T_{OP,B}$. To achieve this revenue, the conversion should be X_B, and the inlet and outlet temperatures should be adjusted to T_B and T_{0B}, respectively. Correspondingly, $\dot{Q}_{UCC}$ will increase to $\dot{Q}_{1B}$, while $\dot{Q}_{UCH}$ decreases to $\dot{Q}_{2B}$.

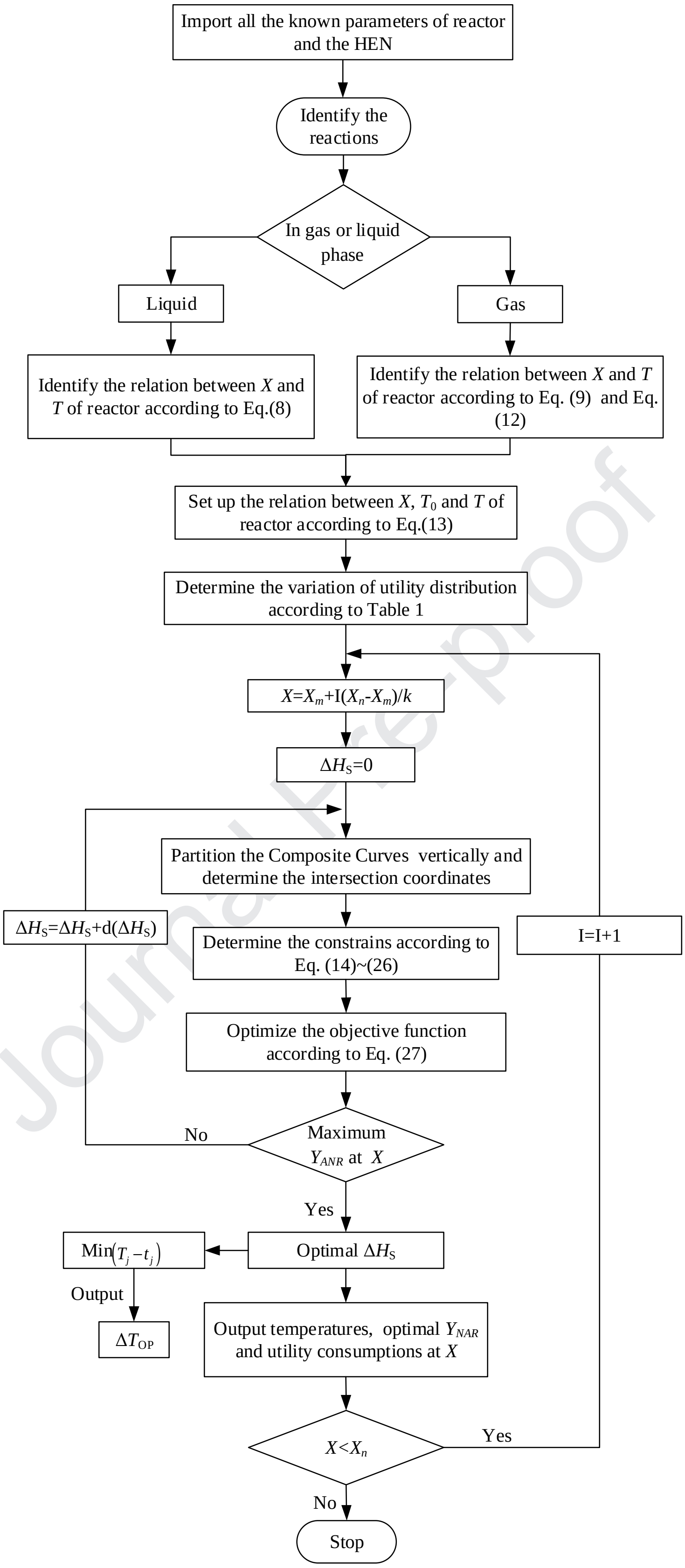

Fig. 7 Flowchart for optimizing the conversion of CSTR reactor

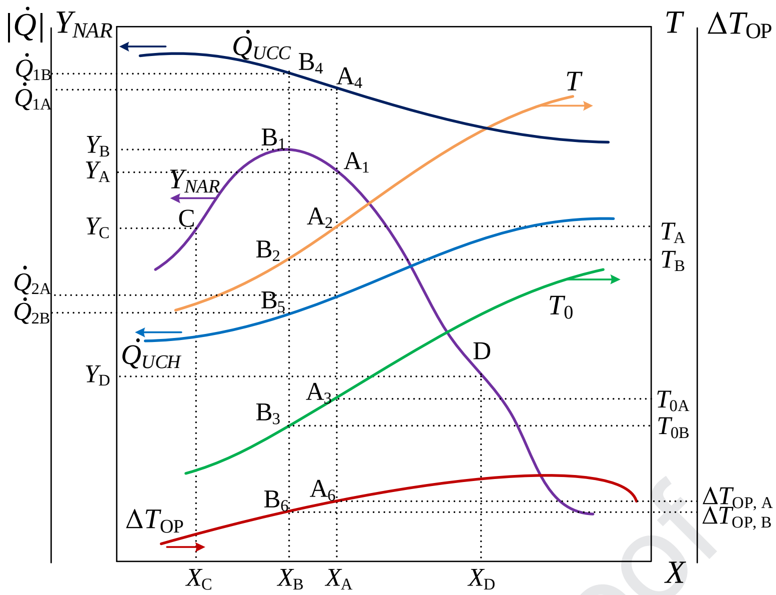

Fig. 8 The $\dot{Q}$-Y_{NAR}-T-X diagram

3 Case Study

3.1 Steam-reforming Process and Its Mathematical Model

The steam-reforming process of an ammonia synthesis plant [57] produces hydrogen for synthesizing ammonia; its simplified flowsheet is illustrated by Fig. 9. The feed of this process includes hydrogen, water, carbon dioxide and carbon monoxide, and their flow rates are 2,914.82 kmol·h^{-1}, 9,562.89 kmol·h^{-1}, 1,271.71 kmol·h^{-1} and 3,875.39 kmol·h^{-1}, respectively. In the current system, the Minimum Temperature Approach is 171 K, and the net revenue is 4,387,000 USD per year. According to the design data of this plant, the total heat exchange area of HEN is 812 m^2.

Hydrogen is produced in the adiabatic CSTR reactor, R1501, and the main reaction is as following:

$$H_2O(g)+CO(g) \rightleftharpoons H_2(g)+CO_2(g)$$

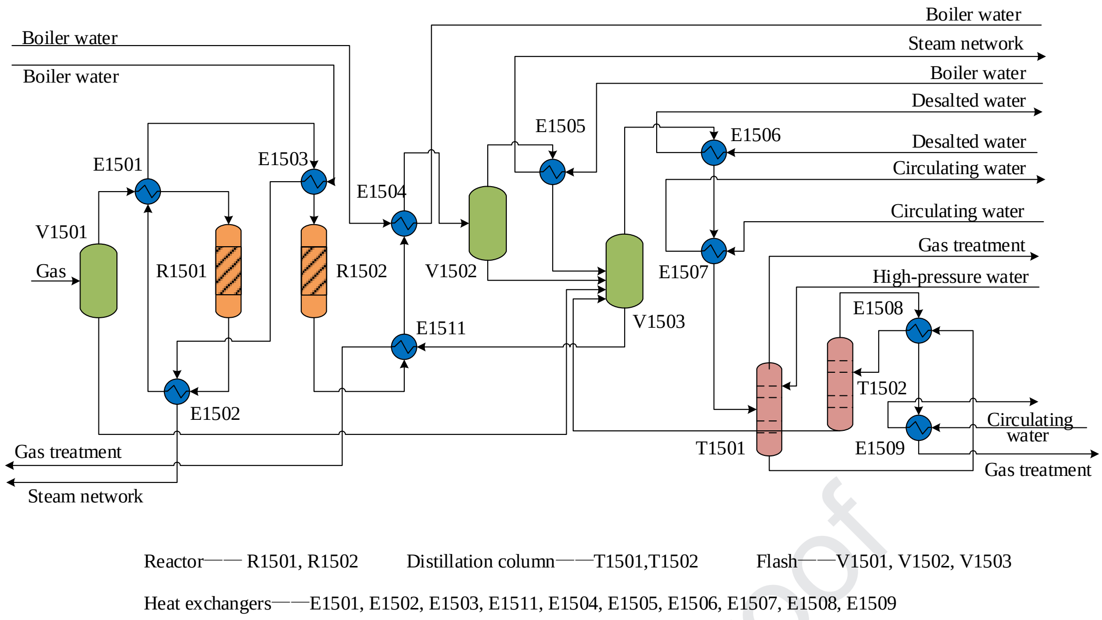

Fig. 9 Flowsheet of a steam-reforming process

When R1501 is operated at high pressure (>2.5 MPa) and high temperature (>600 K) with 112g·m^{-3} of B113-2 catalyst, the reaction rate (r) of the key component, CO, is represented by Eq. (28) [57].

$$-r_{\mathrm{CO,\,2.5MPa}} = 119.7\exp(-46{,}286/RT)P_{\mathrm{CO}}^{0.7660}P_{\mathrm{H_2O}}^{0.3335}P_{\mathrm{CO_2}}^{-0.3696}P_{\mathrm{H_2}}^{0.0936}(1-\omega) \tag{28}$$

Where, $r_{\mathrm{CO,2.5MPa}}$ is the reaction rate of CO at 2.5 MPa, mol·h^{-1}·m^{-3}; ω is approximately taken as zero [50], and this is feasible when the temperature and pressure are greater than 600 K and 2.5 MPa, respectively.

When the reactor's pressure is greater than 1.0 MPa, the reaction rate is proportional to the pressure of the system [57]. Based on this, the reaction rate of CO at 5.65 MPa is obtained by revising the coefficient of Eq. (28), and is shown by Eq. (29).

$$-r_{\mathrm{CO,\,5.65MPa}} = 270.52\exp(-46{,}286/RT)P_{\mathrm{CO}}^{0.7660}P_{\mathrm{H_2O}}^{0.3335}P_{\mathrm{CO_2}}^{-0.3696}P_{\mathrm{H_2}}^{0.0936}(1-\omega) \tag{29}$$

Furthermore, the partial pressure of water, hydrogen and carbondioxide are calculated by Eq. (30), Eq. (31) and Eq. (32), respectively.

$$P_{H_2O} = P^{total}\cdot y_{H_2O} = P^{total}\cdot\frac{F_{H_2O}^{0} - F_{\mathrm{CO}}^{0}\cdot X}{F} \tag{30}$$

$$P_{H_2} = P^{total} \cdot y_{H_2} = P^{total} \cdot \frac{F_{H_2}^0 + F_{\mathrm{CO}}^0 \cdot X}{F} \tag{31}$$

$$P_{CO_2} = P^{total} \cdot y_{CO_2} = P^{total} \cdot \frac{F_{CO_2}^0 - F_{\mathrm{CO}}^0 \cdot X}{F} \tag{32}$$

When V is 200 m^3, Eq. (33) is derived according to Eq. (10).

$$\exp(-515.52 / T) = 5.23 \times 10^{-9} \frac{(0.178 + 0.543X)^{0.3696} (0.408 + 0.543X)^{0.0936}}{\left[0.534(1-X)\right]^{0.7660} (1.34 - 0.543X)^{0.3335}} \tag{33}$$

With the reaction heat taken as -41,160 J·mol^{-1} at 298.15 K [57] and the heat added to the reactor taken as zero, Eq. (34) is obtained according to Eq. (13).

$$T_0 = T - X \cdot \frac{41{,}160 - 11.07(T - 298.15)}{169.88} \tag{34}$$

The relationships among the inlet temperature, outlet temperature and conversion are obtained according to Eq. (33) and Eq. (34). For this type of catalyst, the conversion of CO usually varies from 0.7 to 0.85 [58].

In the HEN of this process, there are 3 cold streams and 5 hot streams. To consider the variation of CP along temperature, hot stream SR_1, SR_2, SR_4 and SR_5 are divided into multiple sub-streams lying in different temperature intervals. The CP of each sub-stream is taken as a constant, and different sub-streams have different CPs. When the conversion of CO equals 0.79, the data of each stream are listed in Table 2. SK_1 is the feed of R1501, while SR_1 is its outlet product. When the temperature approach is taken as 10 K, the Composite Curves are shown by Fig. 10. In this figure, the main inflection points are marked with letters. It is identified that the HEN is a Threshold Problem with the Threshold Temperature Approach equals 171 K, and the cold utility consumption is 125,241 kW.

Table 2 Data of streams

Stream*	Sub-stream	Heat exchanger	Temperature		Heat flow, kW	*CP*, kW·K^{-1}	*K*, kW·K^{-1}·m^{-2}
			Supply, K	Target, K			
SK_1	-	E1501	504.15	539.15	7,268.75	207.68	2.5
SK_2	-	E1511	447.15	493.15	5,170.87	112.41	1
SK_3	-	E1508	309.15	361.15	3,738.19	71.89	0.8
SR_1	1	E1502	705.15	682.65	4,267.79	189.68	1.4
	2	E1501	682.65	644.45	7,231.87	189.32	2.5
	3	E1503	644.45	518.15	23,888.00	189.14	1.3
SR_2	1	E1511	513.15	488.15	5,170.87	206.83	1.1
	2	E1504	488.15	465.15	18,147.40	789.02	2
SR_3	-	E1505	465.15	437.05	32,259.30	1,148.02	1.2
SR_4	1	E1506	436.15	368.15	32,687.80	480.7	2.3
	2	E1507	368.15	313.15	12,658.30	230.15	1
SR_5	1	E1508	389.35	373.35	3,738.19	233.64	0.8
	2	E1509	373.35	345.15	1,477.99	52.79	1.1

* SK denote cold streams, SR denote hot streams.

According to the traditional analysis method for Threshold HEN [7], the trade-off between capital cost and utility cost is plotted in Fig.11. When the conversion of CO is 0.79, the annual profit of the process keeps unchanged. The net annual revenue equals to the difference between the annual profit and total cost and is represented by the left vertical axis in Fig. 11. In this figure, it is identified that the optimum point lies at the Threshold Temperature Approach (171 K) and the maximum net annual revenue is 4,387,000 USD per year. These data are in good agreement with those of the current process. This means that the current process corresponds to the maximum net annual revenue identified by the traditional optimization method.

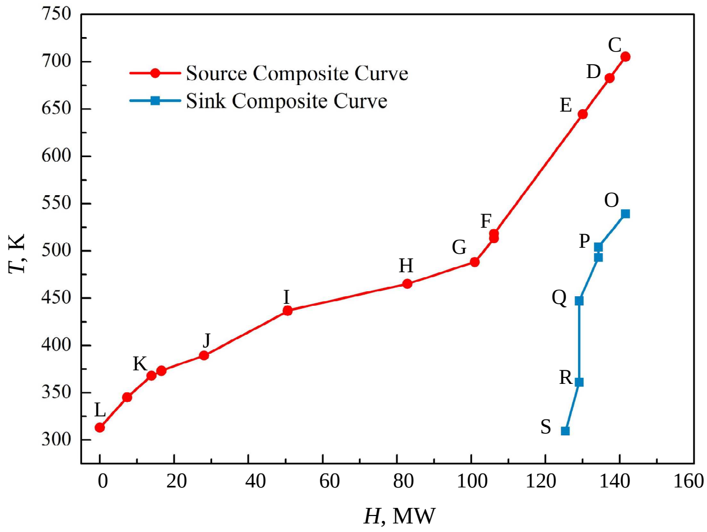

Fig. 10 Composite curves when the conversion of CO is 0.79

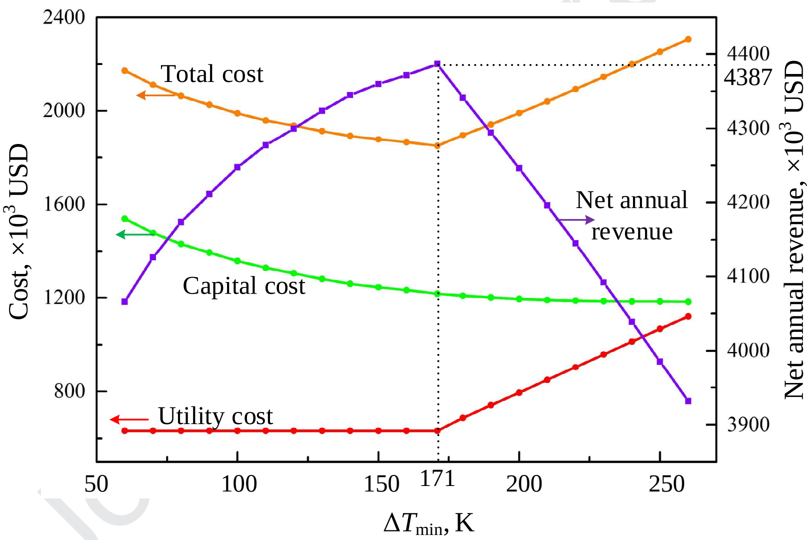

Fig. 11 Trade-off between capital and utility costs (traditional analysis method)

In Fig. 10, point C and O correspond to the supply temperature of SR_1-1 and target temperature of SK_1, respectively. According to Table 1, the duty variation for the Sink and Source Composite Curves, ΔH_1 and ΔH_2, are calculated by Eq. (35) and Eq. (36), respectively. And, the variation of heating and cooling utility are determined by Eq. (37) and Eq. (38).

$$\Delta H_1 = 207.68 \times \left(T_0' - 539.15\right) \tag{35}$$

$$\Delta H_2 = 189.68 \times \left(T' - 709.15\right) + 11.07 X' \left(T' - 682.65\right) \tag{36}$$

$$\Delta\dot{Q}_{\mathrm{HT}} = 207.68T_0' - 189.68T' - 11.07X'T' + 7556.9X' - \Delta H_{\mathrm{S}} + 22551.3 \tag{37}$$

$$\Delta\dot{Q}_{\mathrm{CL}} = -\Delta H_{\mathrm{S}} \tag{38}$$

With the cost of pipeline, meters and the steam generator considered, the increment of annual capital cost is calculated by Eq. (39) [57].

$$Y_{IAC} = 0.0105 Area'^{1.2} - 11.7 \tag{39}$$

For this process, the price of cooling water is 0.074 USD per ton, while that of steam and product are 17.6 USD and 2,205.8 USD per ton. With the operating time and depreciable period taken as 8000 hours per year and 10 years, respectively, the net annual revenue of this vapor transform process is indicated by Eq. (40).

$$Y_{ANR} = 28.66T_0' - 26.18T' + 0.141\Delta H_{\mathrm{S}} + 97X' - 0.0105Area'^{1.2} - 0.35T'X' - 3171 \tag{40}$$

According to equations (28)~(40) and the optimization procedure shown in Fig. 7, the mathematical model of this system is built and solved by Matlab R2018a, and the results are obtained in 27s (CPU i5-7500, RAM 8G).

3.2 Results and Discussion

On the basis of optimization, the maximum net annual revenues at different conversions are obtained, and the $\dot{Q}$-Y_{NAR}-T-X diagram, Fig. 12, is plotted. This figure shows that the reactor's inlet and outlet temperature increases along conversion, and the Minimum Temperature Approach corresponding the optimal revenue keeps to be 10 K when the conversion changes in interval [0.70, 0.85]. The reason is that both the varying sink and source lie above the Threshold Temperature Approach (point P), and the Minimum Temperature Approach always lies at point P when the Sink Composite Curve is shifted. Consequently, the modified distance (ΔH_{S}) for the Sink Composite Curves remains to be 27,885 kW at different conversions.

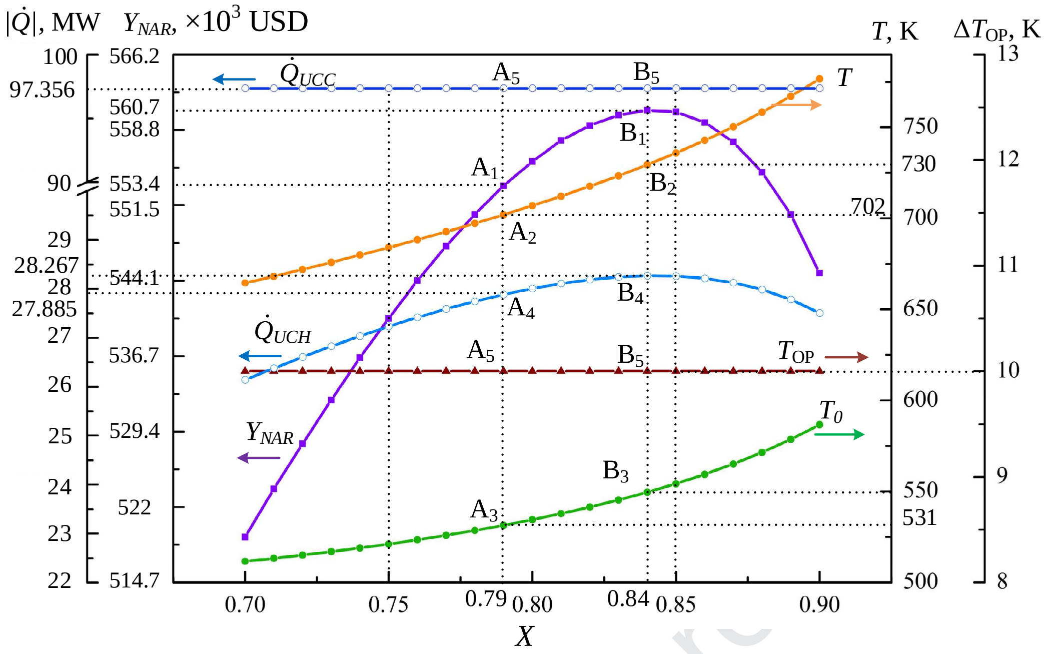

Fig. 12 The $\dot{Q}$-Y_{NAR}-T-X diagram of the steam transform process

For a given conversion, the optimal revenue and corresponding reactor parameters can be identified from this figure. When the reactor is operated at conversion 0.79, the inlet and outlet temperature corresponds point A_3 and A_2, and are 531 K and 702 K, respectively. These values are in good agreement with the practical values. The optimal revenue is identified to be 5,534,000 USD per year, 26.15% more than that of the current process (4,387,000 USD per year). The reason causing such a significant reduction of revenue is the optimization of the Minimum Temperature Approach. By the proposed method, the Minimum Temperature Approach is identified to be 10 K, instead of the 171 K (identified by the traditional pinch method). As the Minimum Temperature Approach decreases to 10 K, the capital cost of the HEN increases, the cooling utility decreases significantly, and more energy at the hot end of Composite Curves is recovered to generate steam. The revenue of steam and the reduced cooling utility is much greater than the increment of capital cost. Because of this, the net annual revenue identified by the proposed method is 26.15 % more than that identified by the traditional pinch method.

Within the conversion interval [0.7, 0.85], the revenue increases first and reaches the maximum value when conversion equals 0.84, while it decreases when the conversion increases from 0.84 to 0.85. In Fig. 12, it is identified that the variation of the net annual revenue is consistent with that of the energy recovered at the hot end, which demonstrates that heat recovery is the main factor affecting the net annual revenue of this process.

At conversion 0.84, the net annual revenue reaches the maximum, 5,607,000 USD per year, 27.82 % more than that of the current process, and 1.67 % more than that at conversion 0.79. Therefore, the optimal conversion of the reactor is 0.84, and the corresponding Optimal Temperature Approach is still 10 K. Table 3 compares the current utility consumptions and the annual revenue, with those identified by the traditional pinch method and the proposed method. With the proposed method, it can be seen that the maximum net annual revenue at conversion 0.79 is 1.67 % less than that at conversion 0.84. The reason is that at conversion 0.84, the heat recovered for generating steam reaches the maximum at the hot end of the Composite Curves. Correspondingly, the minimum cooling utility consumption and the maximum net annual revenue are obtained at this conversion, as shown by Table 3 and Fig. 12.

To verify the accuracy of the results, the Composite Curves corresponding the optimal conversion (0.84) and the Optimal Temperature Approach (10 K) is plotted in Fig. 13. In this figure, the Minimum Temperature Approach appears at the dash line. The variations of $\dot{Q}_{UCC}$ and $\dot{Q}_{UCH}$ are 27,885 kW and 28,267 kW, respectively, and are in good agreement with the results identified by proposed method. Therefore, the proposed method can be applied to optimize the HEN and reactor.

Table 3 Comparison for different methods

Parameters, consumptions and revenue	Current value/Optimum value identified by the traditional method	Optimum value identified by the proposed method	
Conversion of R1501	0.79	0.79	0.84
Outlet temperature of R1501, K	702	702	730
Cooling utility, kW	125,241	97,365	97,365
Optimal ΔH_S, kW	-	27,885	27,885
Threshold Temperature Approach, K	171	10	10
Duty for producing steam, kW	0	27,885	28,267
Product yield, $t \cdot year^{-1}$	48,985	48,985	52,085
Net annual revenue, USD	4,387,000	5,534,000	5,607,000
Increment	-	26.15%	27.82%

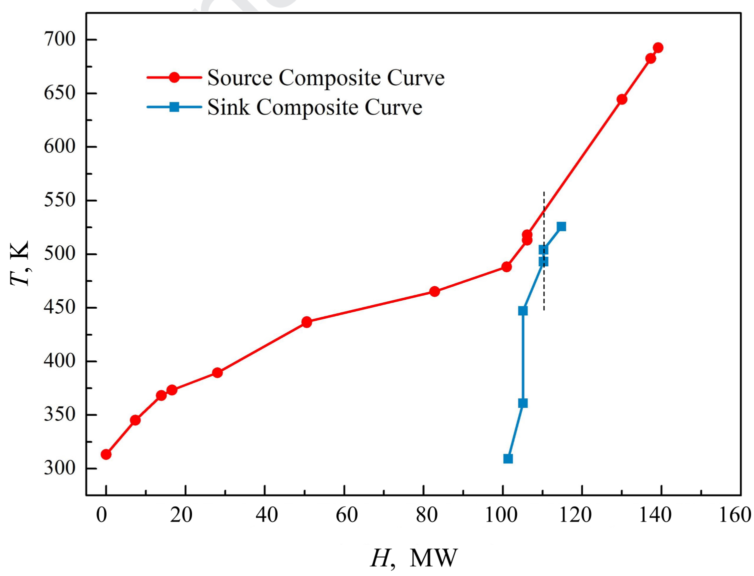

Fig. 13 The Composite Curves when the conversion of CO is 0.84

Fig. 12 shows that, the Optimal Temperature Approach (T_{OP}) keeps to be 10 K as the conversion change, the cooling utility consumption keeps unchanged and the capital cost changes slightly. When the Optimal Temperature Approach changes along the conversion, the cooling utility consumption and capital cost will change significantly, and there might be multiple extreme points at the net annual revenue curve. Although this situation is complex than the case studied in this section, the maximum net annual revenue can also be identified from the $\dot{Q}$-Y_{NAR}-T-X diagram, as well as the corresponding Optimal Temperature Approach and reactor parameters (including the inlet and outlet temperatures, conversion).

4 Conclusions and Future Work

In this paper, a combined Pinch and Mathematical Programming Methodology is proposed to systematically analyze the integration of Threshold HEN and CSTR reactor. The proposed model can be used to optimize the HEN and CSTR reactors with the capital cost and utility cost considered simultaneously. The $\dot{Q}$-Y_{NAR}-T-X diagram illustrates the variation of the net annual revenue, the reactor's temperature and the minimum temperature approach clearly, and can be used to target their values at different conversions, and identify the optimal conversion and the corresponding reactor temperature and revenue. The proposed method can be used to integrate the HEN with CSTR reactor, and optimize the minimum temperature approach and reactor parameters.

For the studied case, the maximum net revenue is identified to be 5,607,000 USD per year, 27.82 % and 1.67 % more than that identified by the traditional method and the proposed method at conversion 0.79. The optimal conversion and minimum temperature approach for achieving the maximum net revenue are 0.84 and 10 K, respectively. Case study shows that HEN and reactor can be optimized by the proposed method efficiently and accurately.

In the proposed method, only single reaction and CSTR reactor are considered. For the integration of HEN with PFR/Batch reactors and multiple reaction systems, integral equations and implicit function equations should be included in the mathematical model, and its solving is much more complex. The proposed method cannot be applied directly, and should be extended with the difference between single and multiple reactions, and that between CSTR and PFR/Batch reactors incorporated. Based on the work in this manuscript, this will be investigated in the future.

Acknowledgement

Financial supports provided by the National Natural Science Foundation of China (21736008) and (U1662126) are gratefully acknowledged.

Nomenclature

Indices

j	Heat flow interval
Sets	
$[X_m, X_n]$	Operating conversion interval of reactor
$[1, J]$	Range of heat flow interval
Parameters	
a, b and u	Constants related to heat exchanger cost
CP	Heat capacity flow rate, $kW \cdot K^{-1}$
D_P	Depreciable period for heat exchangers, year
D_T	Annual operating time, $h \cdot year^{-1}$

F	Total inlet molar flow rate of reactor, $kmol \cdot h^{-1}$
F_i^0	Inlet flow rate of species i, $kmol \cdot h^{-1}$
J_C	Unit price of cooling utility, $USD \cdot ton^{-1}$
J_P	Unit price of product, $USD \cdot ton^{-1}$
J_Q	Revenue of unit steam, $USD \cdot ton^{-1}$
J_S	Unit price of heating utility, $USD \cdot ton^{-1}$
K	Overall heat transfer coefficient, $kW \cdot m^{-2} \cdot K^{-1}$
P^{total}	Total pressure of reactor, MPa
$\dot{Q}$	Heat flow of the point on the Source Composite Curve, kW
$\dot{q}$	Heat flow of the point on the Sink Composite Curve, kW
T	Temperature of hot streams, K
t	Temperature of cold streams, K
V	Reactor volume, m^3
W_C	Energy provided by unit cooling utility, $kJ \cdot ton^{-1}$
W_Q	Energy consumption demanded to produce unit steam, $kJ \cdot ton^{-1}$
W_S	Energy provided by unit heating utility, $kJ \cdot ton^{-1}$
Y_{eq}	Installation cost, USD
z	Installation factor of heat exchanger
ΔT_{min}	Minimum temperature approach allowed by the chemical process, K
ω	Reversibility factor

Variables

$Area$	Heat transfer area, m^2
P_i	Partial pressure of species i in reactor, MPa
X	Conversion of the key component in reactor

Y_{AHR}	Annual heat recovery, USD·year^{-1}
Y_{APV}	Annual product variation of the product, USD·year^{-1}
Y_{IAC}	Annual increment of capital cost, USD·year^{-1}
Y_{NAR}	Net annual revenue, USD·year^{-1}
y_i	Mole fraction of species *i* in reactor
ΔH_{S}	Leftwards shifted distance for the Sink Composite Curves, kW
$\Delta\dot{Q}_{\mathrm{CL}}$	Duty variation of cooling utility, kW
$\Delta\dot{Q}_{\mathrm{HT}}$	Duty variation of heating utility, kW
$\Delta\dot{Q}_j$	Duty variation in vertical interval *j*, kW
ΔT_{OP}	Optimal temperature approach, K

Others

A	Pre-exponential factor
c_i	Concentration of species *i* , mol·m^{-3}
Cp	Heat capacity, kJ·mol^{-1}·K^{-1}
CP	Heat capacity flow rate, kJ·h^{-1}·K^{-1}
E	Activity energy, kJ
F_i	Outlet molar flow rate of species *i*, kmol·h^{-1}
G	Factor related to reverse reaction
H	Heat flow of hot/cold streams, kW
i	Species *i* in the reaction system
k	Reaction rate constant
$\dot{Q}_{\mathrm{Cmin}}$	Duty of minimum cooling utility, kW
$\dot{Q}_{\mathrm{Hmin}}$	Duty of minimum heating utility, kW
$\dot{Q}_{\mathrm{R}}$	Energy supplied to the reactor, kW

$\dot{Q}_{UCC}$	Surplus or deficient load at the cold end of Composite Curves, kW
$\dot{Q}_{UCH}$	Surplus or deficient load at the hot end of Composite Curves, kW
r	Reaction rate, $mol \cdot m^{-3} \cdot h^{-1}$
SR_p	Hot stream corresponding to the feed of the reactor
SK_q	Cold stream corresponding to the product of the reactor
T_R	Reference temperature, K
T_0	Inlet temperature of reactor, K
α_i	Stoichiometric number of species i in the reaction
ξ_i	Stoichiometric coefficient for species $i$in the reaction
ΔH_1	Duty variation of the outlet stream of the reactor, kW
ΔH_2	Duty variation of the inlet stream of the reactor, kW
ΔH_{Rx}^{Θ}	Reaction heat, $kJ \cdot mol^{-1}$
ΔT_THR	Threshold Temperature Approach, K

Abbreviations

AHP	Analytic Hierarchy Process
CSTR	Continuous Stirred Tank Reactor
HEN	Heat Exchanger Network
LMTD	Logarithmic Mean Temperature Difference
MCS	Monte Carlo Simulation
MINLP	Mixed Integer Nonlinear Programming
MP	Mathematical Programming
PFR	Plug Flow Reactor
SePTA	Segregated Problem Table Algorithm

References

[1] J.I. Chowdhury, Y. Hu, I. Haltas, N. Balta-Ozkan, G. Jr. Matthew, L. Varga. Reducing industrial energy demand in the UK: A review of energy efficiency technologies and energy saving potential in selected sectors. Renewable and Sustainable Energy Reviews. 94 (2018) 1153-1178.

[2] U.S. Energy Data. U.S. Energy Information Administration, 2018. http://www.eia.doe.gov.

[3] BP Satatistical Review of World Energy. 2018, 67th Edition, BP p.l.c., London, UK.

[4] S. Kilkis, G. Krajačić, N. Duić, M.A. Rosen, M.d.A. Al-Nimr. Advancements in sustainable development of energy, water and environment systems. Energy Conversion and Management. 176 (2018) 164-183.

[5] D. Zhang, P. Wang, G. Liu. A novel sensitivity analysis method for the energy consumption of coupled reactor and heat exchanger network system. Energy & Fuels. 32 (2018) 7210-7219.

[6] D. Zhang, G. Liu, Y. Li. Graphical optimization method for coupled heat exchanger network and reactor. Energy. 156 (2018) 635-646.

[7] R. Smith. Chemical Process Design and Integration. 2010, 2nd Edition, Chichester: John Wiley,.

[8] B. Linnhoff, J.R. Flower. Synthesis of heat exchanger networks: II. Evolutionary generation of networks with various criteria of optimality. AIChE Journal. 24 (1978) 642-654.

[9] B. Linnhoff, E. Hindmarsh. The pinch design method for heat exchanger networks. Chemical Engineering Science. 38 (1983) 745-763.

[10] B. Bakhtiari, S. Bedard. Retrofitting heat exchanger networks using a modified network pinch approach. Applied Thermal Engineering. 51 (2013) 973-979.

[11] M.A. Gadalla. A new graphical method for Pinch Analysis applications: Heat exchanger network retrofit and energy integration. Energy. 81 (2015) 159-174.

[12] L. Kang, Y. Liu, N. Jiang. Synthesis of large-scale heat exchanger networks using a T-Q diagram method. Canadian Journal of Chemical Engineering. 94 (2016) 1955-1964.

[13] B. Li, Y. C. Castillob, C. Chang. An improved design method for retrofitting industrial heat exchanger networks based on Pinch Analysis. Chemical Engineering Research and Design. 148 (2019) 260–270.

[14] V.P. Leandro, B. Caliane, A. Mauro. Work and heat exchange network synthesis considering multiple electricity-related scenarios. Energy. 182 (2019) 932-953.

[15] S. Hwangbo, K. Nam, J. Han. Integrated hydrogen supply networks for waste biogas upgrading

and hybrid carbon-hydrogen pinch analysis under hydrogen demand uncertainty. Applied Thermal Engineering. 140 (2018) 386-397.

[16] M. Souifi, A. Souissi. Simultaneous water and energy saving in cooling water networks using pinch approach. Materials Today: Proceedings. 13(2019) 1115-1124.

[17] R.R. Tan, K.B. Aviso, D.C.Y. Foo. Carbon emissions pinch analysis of economic systems. Journal of Cleaner Production. 182(2018) 863-871.

[18] R. Smith, M. Jobson, L. Chen. Recent development in the retrofit of heat exchanger networks. Applied Thermal Engineering. 30 (2010) 2281-2289.

[19] M. Garbs. Pinch analysis and process integration: a user guide on process integration for the efficient use of energy[J]. Journal of Cleaner Production. 110(2016) 203-212.

[20] Z. Wei, L. Sun, Z. Yuan, R. Jiang. Design and application of heat exchanger network for a hot-end threshold problem. Acta Petrolei Sinica (Petroluem Progressing Section). 30 (2014) 748-55

[21] M.H. Panjeshahi, E.G. Langeroudi, N. Tahouni. Retrofit of ammonia plant for improving energy efficiency. Enery. 33 (2008) 46-64.

[22] G. Ashkan, S. Mehdi. Optimization of the energy consumption in the industrial cycle of soot production using pinch technology. Recent Advances in Fluid Mechanics and Heat & Mass Transfer. 20(2011): 61-67.

[23] M. Wang, L.N. Gong, J. L.Li. Energy recovery in process of acetic acid cracking. Chemical Engineering (Chinese). 42 (2014) 1-5.

[24] L. Sun, X. Luo, Y.Zhao. Synthesis of multipass heat exchanger network with the optimal number of shells and tubes based on pinch technology. Chemical Engineering Research and Design. 93(2015) 185-193.

[25] J. Klemeš, P. Varbanov. Process Integration: pinch analysis and mathematical programming - directions for future development. Computer Aided Chemical Engineering. 38(2016) 2405-2406.

[26] R. Srikanth, R.H. Joga, G. Kalyani. Optimization of heat exchanger network in crude distillation unit for an existing refinery using pinch technology. Research Journal of Pharmaceutical. Biological and Chemical Sciences. 8(2017) 485-496.

[27] X. Liu, X. Luo, S. Kabelac. Studies on a novel optimal retrofit strategy of heat exchanger networks applied in crude oil distillation unit. Industrial& Engineering Chemistry Research. 55

(2016) 11283-11290.

[28] S. R. Wan Alwi, Z. A. Manan , M. Misman, C. Wei Sze. SePTA—A new numerical tool for simultaneous targeting and design of heat exchanger networks. Computers&Chemical Engineering. 57 (2013) 30-47.

[29] C. Zhang, G. Cui, F. Peng. A novel hybrid chaotic ant swarm algorithm for heat exchanger networks synthesis. Applied Thermal Engineering. 104 (2016) 707-719.

[30] L.V. Pavão, C.B.B. Costa, M.A.S.S. Ravagnani. A new stage-wise superstructure for heat exchanger network synthesis considering substages, sub-splits and cross flows. Applied Thermal Engineering. 143 (2018), 719-735.

[31] N. Jiang, W. Han, F. Guo, H. Yu, Y. Xu, N. Mao. A novel heat exchanger network retrofit approach based on performance reassessment. Energy Conversion and Management. 177(2018), 477-492.

[32] Y. Q. Lai, Z. A. Manan, S. R. Wan Alwi. Simultaneous diagnosis and retrofit of heat exchanger network via individual process stream mapping. Energy. 155 (2018) 1113-1128.

[33] N. S. Lai, M. J. Atkins, T. G. Walmsley, M. R.W. Walmsley, J. R. Neale. Insightful heat exchanger network retrofit design using Monte Carlo Simulation. Energy. 181 (2019) 1129-1141.

[34] F. Liu, J. Ma, X. Feng. Simultaneous integrated design for heat exchanger network and cooling water system. Applied Thermal Engineering. 128(2017) 1510-1519.

[35] E. Martelli, C. Elsido, A. Mian, F. Marechal. MINLP model and two-stage algorithm for the simultaneous synthesis of heat exchanger networks, utility systems and heat recovery cycles. Computers and Chemical Engineering. 106 (2017) 663–689.

[36] T. B. Mano, G. Guillén-Gosálbez, L. Jiménez , M.A.S.S. Ravagnani. Synthesis of heat exchanger networks with economic and environmental assessment using fuzzy-Analytic Hierarchy Process, Chemical Engineering Science. 195 (2019) 185–200.

[37] X. Hong, Z. Liao, J. Sun, B. Jiang, J. Wang, Y. Yang. Transshipment type heat exchanger network model for intra- and inter-plant heat integration using process streams. Energy. 178 (2019) 853-866.

[38] L. Liu, Y. Bai, L. Zhang, S. Gu, J. Du. Synthesis of flexible heat exchanger networks Considering gradually accumulated deposit and cleaning management. Industrial & Engineering Chemistry Research. 58(2019) 12124−12136.

[39] S. Gu, L. Liu, Lei Zhang, Y. Bai, J. Du. Optimization-based framework for designing dynamic flexible heat exchanger networks. Industrial & Engineering Chemistry Research. 58(2019) 6026−6041.

[40] C. B. Malham, R. Riveratinoco, Z.Assaad, D. Chretien, M. Riche, N. Guintrand.. A novel hybrid exergy/pinch process integration methodology. Energy.156 (2018): 586-596.

[41] H. Zhang, G. Cui, Y. Zhu, X. Huang. Optimization and analysis of specific heat exchanger network cases. Chemical IndustryEngineering Progress (China). 37 (2018) 1692-1700.

[42] K.N. Sun, S.R. Wan Alwi, Z.A. Manan. Heat exchanger network cost optimization considering multiple utilities and different types of heat exchangers. Computer Chemical Engineering. 49 (2013) 194-204.

[43] S.H.A. Bakar, M.K.A. Hamid, S.R. Wan Alwi, Z.A. Manan. Selection of minimum temperature difference (DTmin) for heat exchanger network synthesis based on trade-off plot. Applied Energy. 162 (2016) 1259-1271.

[44] P. Glavič, Z. Kravanja, M. Homšak. Heat integration of reactors—I. Criteria for the placement of reactors into process flowsheet. Chemical Engineering Science. 43 (1988) 593-608.

[45] Z. Kravanja, P. Glavič. Heat integration of reactors—II. Total flowsheet integration. Chemical Engineering Science. 44 (1989) 2667-2682.

[46] X. Tian, C. Yin, D. Lv, P. Wang, G. Liu. Effect of catalyst deactivation on the energy consumption of gasoline–diesel hydrotreating process. Energy & Fuels. 32 (2018) 10879-10890.

[47] L.B. Director, V.A. Sinelshchikov. Numerical modeling of torrefaction reactor integrated in energy technological complex. Energy. 167 (2019) 1194-1204.

[48] M. Kim, J. Park, S. Yu, C. Ryu, J. Park. Clean and energy-efficient mass production of biochar by process integration: Evaluation of process concept. Chemical Engineering Journal. 355 (2019) 840-849.

[49] H.S. Fogler. Elements of chemical reaction engineering. Pearson Education,Prentice-Hall.New Jersey, American.4th Edition (2006).

[50] Q.S. Liu, F.J. Zhao, Z.J Mu. The macro-kinetics of water-gas shift reaction on B113-2 shift catalyst. Journal of Inner Mongolia University of Technology (China). 22 (2003) 186-191.

[51] R.L. Keiski, T. Salmi, P. Niemistö, J. Ainassaari, V.J. Pohjola. Stationary and transient kinetics of the high temperature water-gas shift reaction. Applied Catalysis A: General. 137 (1996) 349-370.

[52] D.W. Townsend, B. Linnhoff. Heat and power networks in process design, part II, design procedure for equipment selection and process matching. AIChE Journal. 29 (1983) 748-771.[42] E. Kayabasi, H. Kurt. Simulation of heat exchangers and heat exchanger networks with an economic aspect. Engineering Science Technology. 21 (2018) 70-76.

[53] Y. Xu, F. Guo, M. Song, N. Jiang, Q. Wang, G. Chen. Exergetic and economic analyses of a novel modified solar-heat-powered ejection-compression refrigeration cycle comparing with conventional cycle. Energy ConversionandManagement. 168 (2018) 107-118.

[54] N. Jiang, W. Han, F. Guo, H. Yu, Y. Xu, N. Mao. A novel heat exchanger network retrofit approach based on performance reassessment. Energy Conversion and Management. 177 (2018) 477-492.

[55] Y. Wang, R. Smith, J.K. Kim. Heat exchanger network retrofit optimization involving heat transfer enhancement. Applied Thermal Engineering. 43 (2012) 7-13.

[56] N. Jiang, W. Han, F. Guo, H. Yu, Y. Xu, N. Mao. A novel heat exchanger network retrofit approach based on performance reassessment. Energy Conversion and Management. 177 (2018) 477-492.

[57] Z. Zhang, Y. Wang, K. Sun, Y. Shao, L. Zhang, S. Zhang, X. Zhang, Q. Liu, Z. Chen, X. Hu. Steam reforming of acetic acid over Ni–Ba/Al2O3 catalysts: Impacts of barium addition on coking behaviors and formation of reaction intermediates. Journal of Energy Chemistry. 43(2020) 208-219.

[58] Q.S. Liu, F.J. Zhao, Z.J Mu. The macrokinetics of water-gas shift reaction on B113-2 shift catalyst. Journal of Inner Mongolia University of Technology (China). 23 (2004) 103-109.

Research highlights

- A combined Pinch and Mathematical Programming method is proposed.
- Reactor and Threshold HEN are integrated considering reaction kinetics, mass and energy balance.
- A MINLP model is developed with the Minimum Temperature Approach (ΔT_{min}) taken as a variable.
- Diagram is built to target the optimal conversion, ΔT_{min} and reactor parameters.
- The net annual revenue of the steam-reforming process increases by 27.82% after optimization.

Declaration of interests

☒ The authors declare that they have no known competing financial interests or personal relationships that could have appeared to influence the work reported in this paper.

☐The authors declare the following financial interests/personal relationships which may be considered as potential competing interests: